

# **The SST multi-decadal variability in the Atlantic-Mediterranean region and its relation to AMO**

Salvatore Marullo<sup>1</sup>

ENEA, Technical Unit of Development of Applications of Radiations -  
Diagnostics and Metrology Laboratory, Frascati, Italy

Vincenzo Artale

ENEA, Technical Unit of Modelling, Energy and Environment , Roma,  
Italy

Rosalia Santoleri

CNR, Istituto di Fisica dell'Atmosfera e del Clima, Roma, Italy

---

<sup>1</sup> *Corresponding author address:* Salvatore Marullo, ENEA, Via Enrico Fermi 45,  
00044 Frascati, Italia.

E-mail: [salvatore.marullo@enea.it](mailto:salvatore.marullo@enea.it)

## Abstract

Two Sea Surface Temperature (SST) time series, the Extended Reconstructed SST (ERSST.V3) and Hadley Centre Sea Ice and Sea Surface Temperature dataset (HadISST), are used to investigate SST multi-decadal variability in the Mediterranean Sea. The consistency between these two time series and the original International Comprehensive Ocean-Atmosphere Data Set (ICOADS 2.5) over the Mediterranean Sea is investigated, evaluating differences from monthly to multi-decadal scales. From annual to longer time scales, the two time series consistently describe the same trends and multidecadal oscillations and agree with Mediterranean ICOADS SSTs. At monthly time scales the two time series are less consistent with each other, due to the evident annual cycle that characterizes their difference.

The subsequent analysis of the Mediterranean annual SST time series, based on lagged correlation analysis, Multi Taper Method and Singular Spectral Analysis, revealed the presence of a significant oscillation with a period of about 70 years very close to AMO. An extension of the correlation analysis for other world ocean regions confirmed that this multidecadal signal is a unique characteristic of the Mediterranean and North Atlantic Ocean where it reaches its maximum at sub-polar latitudes. North Atlantic indices and Mediterranean SST are significantly correlated and coherent for periods longer than about 40 years.

The results of our analysis are reviewed in the light of the mechanism proposed by Dima and Lohmann (2007) including the role of the Mediterranean Outflow Water in modulating the Atlantic THC and the importance of the Gibraltar strait for the Mediterranean Thermohaline circulation.

## 1. Introduction

Instrumental records of increasing duration and spatial coverage document substantial ocean variability, on timescales ranging from months to decades. Some of this variability can be easily related to known forcing mechanisms, but in many cases the relation between observed variability and forcing is less clear. The same applies to the whole climate system. It has been noted, for example, that this system displays variability on many timescales even in the case of a constant external forcing, i.e., in absence of changes in insolation or atmospheric composition (Dijkstra and Ghil, 2005; Pisacane et al., 2006; Knight et al. 2005; Grist et al., 2009).

The global atmospheric and oceanic circulation has a number of preferred patterns of variability to which correspond specific climate indices. All these have expressions in surface climate fields, that can have a profound regional influence, modulating the location and strength of the local fluxes of heat, moisture and momentum. Classical examples of these “climate modes” are the North Atlantic Oscillation (NAO) (Hurrell, 1995; Trenberth et al., 2007, Knight et al. 2006) and the Atlantic Multi-decadal Oscillation (AMO) (Enfield et al., 2001). The NAO is a leading pattern of weather and climate variability over the Northern Hemisphere that contributes to the redistribution of air masses between the Arctic and the subtropical Atlantic, influencing weather conditions and SST over the Atlantic and adjacent seas. AMO is a climate index which may be defined as the detrended SST anomalies averaged over the North Atlantic from 0°N to 70°N (Enfield et al., 2001). Other definitions of AMO have obtained by

subtracting the global mean SST to remove the large scale global signal that is associated with global processes (Trenberth and Shea, 2006) or by using empirical orthogonal functions (Parker et al. 2007). AMO is characterized by a cycle of about 70 years and has been the object of increasing interest during recent years. There are two main hypotheses about its origin. The first relates this multi-decadal cycle to the internal variability of the thermohaline circulation (THC) and to the intrinsic nonlinear behavior of the climate system (Huck et al., 1999; Delworth and Mann, 2000; te Raa and Dijkstra, 2002, Knight et al., 2005), while the second, based on experimental and numerical evidence brings into play the role of the free oscillation motion of the atmosphere-ocean-ice coupled system (Jungclaus et al., 2005; Dong and Sutton, 2005; Dima and Lohmann, 2007). Recent numerical experiments (Grosfeld et al., 2008) indicate the Atlantic as the main driver for the AMO with a clear coherence between surface air temperature and sea level pressure, exerting influence on the Euro-Atlantic sector. Analysis of the surface temperatures performed by Schlesinger and Ramankutty (1994) suggested that the multi-decadal oscillation arises from predictable internal variability of the ocean-atmosphere system. Analysis of couple models and reconstructed datasets over the global ocean already pointed out the influence of the AMO over the climate of Euro-Atlantic sector (Sutton and Hodson, 2005; Knight et al., 2006; Hodson et al 2009). Sutton and Hodson (2005) documented for the first time the influence of AMO on variations in the summertime climate of both North America and western Europe. Mohino et al. (2010) found that the decadal Sahel rainfall variability is connected to AMO and related positive anomalies over the Mediterranean Sea. No one of these works study in details the Mediterranean

SST multi-decadal variability even if the Mediterranean Sea is often included in their global analysis (eg. Figure 1 of Sutton and Hodson 2005).

The main objective of this paper is to place the Mediterranean Sea at the center of the debate by investigating in detail the multi-decadal variability of the Mediterranean SST field and its relation with the global ocean.

This objective has been pursued using the most recent reconstructed (and non reconstructed) SST datasets (Rayner et al. 2003; Rayner et al. 2006; Smith et al., 2008). Since , recent critical analysis of SST datasets that have highlighted the need of fully validated climatic data records to draw conclusions on trends or low frequency oscillations (Folland and Parker, 1995, Thompson et al. 2008). We first, analyzed the robustness and reliability of the longest instrumental SST time series of the Mediterranean Sea now available (section 2). Then connections between Mediterranean SST and AMO are demonstrated using the Singular Spectral Analysis (SSA) and the Multi Taper Method (MTM) (section 3). Moreover the Mediterranean multi-decadal oscillations are compared with other ocean regions in order to investigate their relevance and correspondences with global scale ocean variability (section 4 and 5). In the concluding section we examine the contribution of the subpolar region on the AMO in the framework of the mechanisms proposed by Dima and Lohmann (2007) and its correlation with the Mediterranean SST. Finally we discuss some speculative but intriguing hypothesis on feedbacks between Mediterranean outflow and the North Atlantic THC based on modeling (Artale et al., 2002; Artale et al., 2006; Calmanti et al., 2006) and observations (Reid, 1979; Lozier and Stewart, 2008).

## 2. Data and methods

### *2.1 The SST Datasets*

The variability of the SST field over the last 150 years has been analyzed using both reconstructed and non-reconstructed SST datasets. One is the International Comprehensive Ocean Atmosphere Data Set (ICOADS) SST version 2.5, that includes all available global surface marine data from 1800 to September 2010 (see Worley et al. 2005 for ICOADS version 2.1 and Woodruff et al. 2010 for ICOADS version 2.5). This dataset consists of monthly summary statistics of several quality checked variables at 1° resolution starting from 1960, and at 2° resolution starting from 1800. The dataset contains data voids where in situ observations were not enough to compute significant monthly statistics.

The ERSST reconstruction uses the ICOADS SST, and is based on a separate analysis of the low- and high-frequency variations. The former are analyzed using a simple average and smoothing of the relatively sparse data, while the analysis of the interannual and shorter-period variations is based on a fitting of observed high-frequency SST anomalies to a set of empirical orthogonal teleconnections (Van den Dool et al., 2000) derived from the more recent spatially complete SST analysis (Smith and Reynolds, 2003; Smith and Reynolds, 2004). In this work we used the updated version 3 (Smith et al., 2008) of the dataset (ERSST.V3) that also includes the adjustment for data before 1941 taking into account differences in measurement practices before that year (Smith and Reynolds 2002).

The third dataset we use is HadISST, that is based on the Met Office Marine Data Bank (MDB) but also includes ICOADS SSTs. In this dataset, sea surface temperatures gaps

are reconstructed using a two stage reduced-space optimal interpolation procedure, followed by superposition of quality-improved gridded observations onto the reconstructions to restore local detail (further details are given in Rayner et al., 2003). HadISST also addresses the problem of the bias in historic SSTs due to changes in SST sampling methods in the 1940s and earlier, using a bias adjustment method proposed by Folland and Parker (1995). ERSST and HadISST use bias-adjusted AVHRR SST beginning in 1985 and 1982 respectively.

## *2.2 Intercomparison of SST datasets over the Mediterranean Sea*

The annual Sea Surface Temperature Anomaly (SSTA) during the last 100-150 years can be more easily estimated using reconstructed SST datasets, such as ERSST and HadISST, that are the most extensively used. However, globally complete, i.e. interpolated, datasets must be used with care (see, e.g., Rayner et al. 2003), particularly in specific regions or periods of time where data are too sparse. Since for most of the time span there is no independent sea “truth” data to validate the reconstructed SST, the only way to evaluate the consistency and quality of the reconstructed time series over particular regions is to inter-compare information extracted from different datasets. Here we have compared the ERSST and HadISST datasets in the Mediterranean region, both on annual and monthly scales, to evaluate differences in long term trends or oscillations and seasonal components. Focusing on the Mediterranean Sea, we notice a good availability of ICOADS (2x2 deg resolution) data for most of the analyzed period (figure 1). In fact, excluding the periods of the two World Wars, during the last century ICOADS observations are available in about 80% of Mediterranean grid boxes or more. This makes the Mediterranean Sea one of the best sampled areas of the world Oceans.

This abundance of data suggests the possibility to estimate the time evolution of the mean sea surface temperature of the Mediterranean Sea directly from the ICOADS SSTs. So the Mediterranean monthly mean time series can be computed by simple space average of all valid ICOADS SST anomalies respect to a mean SST derived from the entire ICOADS record .

As suggested by several authors (Bottomley, 1990; Folland and Parker, 1995), ICOADS SST prior to 1942 have been adjusted using corrections provided by Smith and Reynolds (2002) before any processing step. Smith and Reynolds (2002) showed a general consistency between their corrections and those suggested by Folland and Parker (1995) even though some more marked difference can be observed in winter at high latitudes where the Smith and Reynolds correction is stronger (Smith and Reynolds, 2003).

Starting from monthly ICOADS 2.5 data, yearly averages were computed only for those grid points where 12 monthly values were available for the specific year under examination. In years in which the yearly SST was estimated in less than 15% of the Mediterranean Sea grid points the sea surface temperature was not computed, resulting in data gaps in the annual time series. The 15% limit was empirically fixed after several trials. Figure 2 shows the percentage of grid boxes with yearly averages available in the Mediterranean Sea for each year. Figure 3 compares the three time series for the yearly averages.

The ICOADS SSTs, that are not interpolated, follow quite closely those from the two other series, with differences reaching  $0.2^{\circ}\text{C}$  between 1880 and 1920. The three time series basically describe the same history both in terms of trends and of multidecadal



oscillations, and can consequently interchangeably be used to study the long term variation of the Mediterranean SST field. Moreover the agreement between the two interpolated SST series (ERSST.V3, HadISST) and the non interpolated one suggests that damping or other possible distortions of the interpolation are not dominant in the Mediterranean basin when yearly averages are used.

As shown in figure 4a, on a monthly scale the differences between the two analyses are larger. The differences exhibit a marked annual cycle, suggesting that a form of compensation between seasons may yield the better agreement found for the yearly averages. Similar differences are found between ERSST.V3 and ICOADS (fig. 4b) and HadISST and ICOADS (fig. 4c). Figures 4a and 4c show an increased amplitude of the annual cycle before 1941, when instrumental bias corrections have been applied. A portion of the difference in the amplitude of the annual cycle can possibly be attributed to the different bias adjustment used for the three datasets. Figure 4b, where ERSST and ICOADS are compared, supports this hypothesis, since the difference between these two datasets, that use the same bias correction, are smaller and there is no clear difference between the periods preceding and following 1941.

This inter-comparison does not allow us to identify which of the series is responsible for this annual cycle, but we can still use two additional SST series covering the last three decades to further investigate the problem: the Optimally Interpolated Pathfinder SST (OI\_Path) over the Mediterranean Sea (Marullo et al. 2007) and the Reynolds OIv2 maps based on AVHRR and in situ data (Reynolds et al., 2007) (OIpath and OIv2 hereafter). The validation performed by Marullo et al. (2007) showed that OIPath is able to reproduce in situ measurements with a mean bias of less than 0.1K and RMSE of about

0.5K and that errors do not drift with time (either seasonally or from year to year) or with the percent interpolation error. The absence of any annual cycle in the difference between in situ data and OIPath SSTs makes this dataset the ideal reference to investigate seasonal fluctuation of errors in the reconstructed SST fields.

Reynolds OIv2 are expected to have similar or even better performances being forced to be unbiased with respect to in situ data. Figure 5a and 5b show the differences between the three SST time series under investigation and OIv2 and OIPath, respectively, during the satellite era. Also in this case a clear annual oscillation, with amplitude larger than 0.5 °C, is present. If satellite estimates are free from seasonally oscillating errors as suggested by Marullo et al. (2007), the annual cycle must be attributed to all the reconstructed data sets. This hypothesis is further confirmed by figure 5c where the monthly differences between in situ (obtained by the Coriolis dataset, <http://www.coriolis.eu.org/cdc/dataSelection/cdcDataSelections.asp>) and OIPath satellite data shows that these estimations are free from any annual cycle distortion.

Rayner et al. (2003) have already noted that in the Northern Hemisphere summer, in areas that are well sampled by in situ data, HadISST is systematically warmer than OIv2 SSTs with differences that reach about 0.7 °C in places and suggested that this is symptomatic of a general difference between HadISST and COADS or OIv2. Figures 5a and 5b confirm that, at least in the Mediterranean Sea, a similar bias also occurs between ERSST and OIv2 or OIPath. Some more inference can be achieved by averaging the  $S1=(ERSST-OIPath)$ ,  $S2=(HadISST-OIPath)$  and  $S3 = (all\ in\ situ - OIPath)$  monthly records of figures 5b and 5c to obtain a single mean monthly cycle for each of the three time series. The differences  $S1-S3$  and  $S2-S3$  will approximately represent the mean

monthly bias of ERSST and HadISST reconstruction respect to in situ observations (fig. 6).

While taking into account the limitations of this estimate due to the uneven distribution of the in situ data and to intrinsic differences related to point measurements respect to averages over large boxes or satellite pixels figure 6 reinforces the Rayner et al. (2003) conclusions about the summer HadISST bias and confirms that the same bias also affects ERSST estimates. The mean annual difference between HadISST and in situ and between ERSST and in situ are  $-0.03$  °C and  $0.13$  °C respectively, very close to zero. In conclusion we can state that the three time series are interchangeable and can indifferently be used, depending upon convenience, for climatic studies when averaged over the year to compensate the annual cycle observed in figures 4 and 5, while the monthly time series should be used with more care.

### *2.3 Spectral analysis methods*

We have computed yearly SST averages from ERSST and HadISST for the Mediterranean Sea, for the global ocean and for eight global ocean sub-regions shown in figure 10. Then, annual time series of anomalies with respect to the 1971-2000 mean have been computed, and used to investigate the variability of SST field. Three different methods have been used. First, an autocorrelation analysis was applied to the Mediterranean Sea and to the global ocean ERSST and HadISST anomalies time series, with time lags between 0 to 100 years, to highlight possible multi-decadal oscillation. Then, the time series were also analyzed using the Singular Spectral Analysis (SSA) and the Multi Taper Method (MTM). The SSA technique is a nonparametric spectral estimation method to extract information from short and noisy time series and thus

provides insight into the unknown or only partially known dynamics of the underlying system that generated the series (Broomhead and King, 1986; Fraedrich, 1986; Vautard and Ghil, 1989). This method is based on embedding a time series  $X(t): t = 1, N$  in a vector space of dimension  $M$ . In practice SSA proceeds by diagonalizing the  $M \times M$  lag-covariance matrix  $C_x$  of  $X(t)$  to obtain spectral information on the time series. The entries  $c_{ij}$  of this matrix, that depend only on the lag  $|i-j|$ , are:

$$C_{ij} = \frac{1}{N - |i - j|} \sum_{t=1}^{N - |i - j|} X(t)X(t - |i - j|)$$

The  $M$  eigenvectors  $E_k$  of the lag-covariance matrix  $C_x$  are the temporal empirical orthogonal functions (EOFs). The eigenvalues  $\lambda_k$  of  $C_x$  account for the partial variance in the direction  $E_k$  and the sum of the eigenvalues, gives the total variance of the original time series  $X(t)$ . This is analogous to the classical Principal Component Analysis (PCA) method where the lag-covariance matrix is substituted by the covariance matrix.

SSA can be combined with advanced spectral-analysis methods such as multi-taper method (MTM) to refine the interpretation of oscillatory behavior. In this sense SSA and MTM can be considered complementary. The MTM is a technique developed by D.J. Thomson (1982) to estimate the power spectrum of a stationary ergodic finite-variance random process, which is useful for the analysis of relatively short time series whose spectrum may contain both broadband and line components. The tapering is a solution to approach the leakage problem of finite time series. Classical methods use an unique data taper multiplying a portion of the data at beginning and at the end of the series by an appropriate weighting function. This imply that portions of the time series are excluded from the analysis as a trade-off from reducing spectral leakage in the frequency domain.

MTM uses a small set of tapers rather than a single taper. The data are multiplied by orthogonal tapers constructed to minimize the spectral leakage due to the finite length of the time series. These optimal tapers belong to a family of functions known as "Discrete Prolate Spheroidal Sequences" (DPSS) obtained as eigenvectors of a suitable Rayleigh-Ritz minimization problem (Slepian, 1978). The algorithm to calculate the prolate-Slepian tapers is described by Lees and Park (1995). A detailed description of the MTM is given by Ghil et al. (2002).

To determine whether broadband or line components are present a reshaped spectrum can be determined in which the contributions from harmonic signals are removed (Thomson, 1982; Ghil et al., 2002). The comparison between the reshaped, in which contributions from pure harmonic signals detected by  $F$  variance ratio test with a minimum significance threshold have been removed, and unreshaped MTM gives the opportunity to distinguish signals that are best approximated by harmonic or narrowband oscillations from amplitude and phase modulated and possibly intermittent oscillations.

The use of the MTM implies the choice of the number of tapers ( $K$ ) and the integer bandwidth parameter ( $p$ ). The choice of the bandwidth  $2pf_R$  (where  $f_R$  is the Rayleigh frequency  $1/(N \Delta T)$  with  $N$  number of samples and  $\Delta T$  sampling interval), i.e. the choice of  $p$  and  $K$  is the classical trade-off between spectral resolution and the stability or variance reduction properties of the spectral estimate.

### 3. Analysis of the Mediterranean multi-decadal SST variability

Figure 3 shows that Mediterranean Sea SST time series exhibits a warm phase (positive anomalies respect to the 1971-2000 average) during 1860-1880, 1925-1970 and 1985-today, while a cold phase occurred during 1880-1925, 1970-1985 and presumably before 1860. This suggests that an oscillation with a period of about 70, years, similar to that of the AMO, is also present in the Mediterranean Sea. The occurrence of such an oscillation is confirmed by the lagged autocorrelation plot of figure 7, where a clear maximum for a time lag of 70 years is obtained using both the ERSST and the HadISST temperatures. To get further physical insight and information on the whole spectrum, we then use the SSA and the MTM methods.

We have applied the SSA method to the de-trended Mediterranean ERSST (the longest time series). In order to obtain the signal to noise (S/N) separation we computed and plotted the eigenvalue spectrum of the de-trended time series (Fig 8a). (The detrending was applied to remove any possible deterministic trend leaving mode 1 free, together with mode 2 to explain the multidecadal oscillation (Schlesinger and Ramankutty, 1994). The first two eigenvalues form a pair which contribute about 40% of the total variance and are separated by a very steep slope from the noise, which is characterised by much lower values and a mild slope. The distance of these two modes above the noise indicates that they are deterministic rather than stochastic (Vautard and Ghil, 1989, Vautard et al. 1992). The first two leading EOFs have approximately the same amplitude (considering the range of error bars) and are in quadrature (Fig.8b). Finally, it is worth noting that with only the first two EOFs we capture the main low frequency variability of this SST time

series (Fig. 8c). This fact could be interpreted as the occurrence of a ghost limit cycle related to a physical oscillation of the dynamical system that has generated our SST time series (Ghil et al., 2002).

The low frequency variability of the Mediterranean Sea was also investigated applying the Multi Taper Method (MTM) to the de-trended yearly SST derived from the ERSST.V3 dataset. Following Ghil et al. (2002) we set  $p=2$  and  $K=3$  (less or equal than  $2p-1$ ) as a compromise between the need of resolving decadal scales and the benefit of multiple spectral degrees of freedom. We also de-trended the ERSST.v3 time annual series over the ocean areas under investigation to better distinguish between low frequency bands and the trend.

Figure 8 shows the comparison between the harmonic analysis test (a) and the adaptively weighted estimation (b) against red noise background for the ERSST.v3 series of the Mediterranean Sea. The F test criterion for harmonic signals (fig. 9a) yields 6 peaks at the 99% confidence level and 10 peaks at the 95% confidence level that can eventually be associated to some harmonic, phase-coherent oscillation. Some of the peaks (7.3, 4.3 and 3.2 years) that exceed the 99% confidence level in the harmonic test plot (fig 9a) are associated with very weak power in the spectrum (fig. 9b) while others (73, 6.3, and 2.8 years) correspond to significant spectral bands in the spectrum.

The harmonic test is also useful in the reshaping procedure. Figure 9b shows five peaks that satisfy the harmonic detection test at the 90% level and are also significant relative to the red noise in the spectrum. They include a low frequency band that peaks at 73 years and four higher frequency that peak at 6.3, 3.9, 2.8 and 2.2 years. The higher frequency peaks are very close to the preferred scale of variability of the ENSO's quasi-biennial and

low-frequency modes (Rasmusson et al, 1990; Jiang et al, 1995; Yiou et al, 2000) while the lower frequency is close to that of the AMO. The comparison between the reshaped and the unreshaped spectrum in figure 9b suggests that the four higher frequency peaks (two significantly well above the 99% confidence level and two over the 90% confidence level) are likely to contain a harmonic phase-coherent oscillation with, at least, a 90% level of confidence. The same is not true for the low frequency band at 73 years where the reshaped and the unreshaped spectra are identical. Even if this could be interpreted either as the consequence of the shortness of the SST time series or as the signature of a phase and amplitude modulation or/and an intermittently oscillatory behavior, the multidecadal band is a significant feature of the spectrum. This inference is also supported by the SSA analysis that suggests the physical correspondence of the multidecadal oscillation with some geophysical phenomenon (see figure 8b and related comments).

However some concern still remains about the possibility to truly determine the existence of a 73 year periodicity in a 155 years time series. Previous authors (e.g. Wittenberg, 2009) have verified that century time scale records were not sufficient to resolve the temporal variability of ENSO implying that a different 150 year record could not contain the same oscillation. Having no possibility to extend back in time the instrumental data records one can still investigate if coupled GCM simulations of several hundred of years present plausible scenarios where such or similar multi-decal oscillations are present. To increase the size of our Mediterranean data record we have analyzed, using the same MTM spectral tool, the HadCM3 ( UK Meteorological Office: *Hadley Centre Coupled Model, version 3*) control run which is a coupled atmosphere-



ocean circulation model that have run for 1000 years. This analysis have evidenced, in both harmonic signal F test and MTM spectrum, the presence of a multidecadal peak centered at about 100 years well above the 99% significance level. In this case, the Rayleigh frequency resolution for a harmonic signal resulting from the f test is  $\pm f_R = \pm 1000^{-1}$  cycles/years implies this peak is between 90 and 110 years. At the same frequency the MTM spectrum shows the presence of a narrowband ( $\pm p f_R$  bandwidth) that is likely to contain this harmonic phase-coherent oscillation with a 99% confidence limit. The presence of similar centennial fluctuations of north Atlantic ocean in HadCM3 has been already reported by previous authors (Vellinga and Wu, 2004; Frankcombe et al., 2010).

In the case of the shorter ERSST Mediterranean time series the broader low frequency band contained the 73 years peak of the harmonic analysis test but with Rayleigh frequency resolution of  $\pm 155^{-1}$  cycles/years implying the peak was between 50 and 138 years. Consequently, the two peaks at about 100 and 70 years found in the HadCM3 and in the ERSST time series respectively cannot be considered significantly separated giving the length of the two time series. This result, although is not a definitive proof, is consistent with the hypothesis that also a different 155 years record should contain a similar 70 years peak.

## 4. Mediterranean Sea versus global ocean

The Mediterranean multi-decadal oscillation observed in figure 3 and confirmed by the subsequent time series analysis (section 3), is not evident in the global SSTs time series. The SSA and MTP analysis (not shown) of the global SST time series performed using the same parameter used for the Mediterranean series, do not reveal any significant periodicity in the neighborhood of 70 years. In this case, the first two temporal EOFs, which contribute about 50% of the total variance, suggest the presence of a longer than 70 years period oscillation. The third mode, that only accounts for 10 % of the variance, suggests the occurrence of a periodicity close to 60 years but does not form any pair with the next mode that contributes to the total variance only with a 5%. Using the same approach, Schlesinger and Ramankutty (1994) analyzed a series of near surface global air temperatures from 1854 to 1990. They found a 65-75 year oscillation in the global-mean temperature but argued that this oscillation is the statistical result of a regional long-timescale oscillation that exclusively occurs in the Northern Hemisphere. Considering the close correlation between SST and near surface air temperature, it makes sense to investigate whether a similar spatial distribution of the 70 years long-timescale is also recognizable for the SST field. We expect that this oscillation should be observed at least in the North Atlantic where the AMO is acting.

A first screening can be done applying the lagged autocorrelation procedure used for the Mediterranean Sea to other regions of the oceans. We have divided the oceans in eight boxes (sub-regions) and produced an autocorrelation plot for each of them (fig. 10). The results indicate that the North Atlantic Ocean is the only other area of the world ocean

that clearly exhibits the same oscillation with period of 70 years observed in the Mediterranean Sea.

Since the North Atlantic box covers a wide latitudinal range going from tropical to sub-polar regions, it is interesting to investigate the latitudinal distribution of the low frequency peak, so to quantify the relative role of the polar and of the southern regions in modulating the multidecadal oscillation. To do so, we have applied the MTM analysis to latitudinal bands of  $20^\circ$  in the North Atlantic, that move with steps of  $2^\circ$  from  $10^\circ$  N to  $60^\circ$  N using ERSST data. The latitudinal behavior of the amplitude of low frequency peak resulting from harmonic analysis test of each time series is shown in figure 11. Peaks that exceeds the 99% confidence limit centered between 64 and 73 years are observed only for latitudinal bands north of  $30^\circ$  N with a maximum at  $50^\circ$  N. Note that the difference between the three periods of figure 11 is not significant considering the Rayleigh frequency resolution  $\pm f_R$  ( $f_R = 1/N\Delta T$ ) that results from the annual time series length. All the peaks indicated in figure 11 correspond to significant bands (over 99% confidence limit) in the power spectrum then, even if the harmonic test alone do not definitively proves the existence of a particular oscillation, the simultaneous existence of harmonic signals and spectrum bands that satisfy a 99% confidence limit is a strong indication that such an oscillation exists. In addition the qualitative analysis of the time series plots (fig. 10) further supports such an assumption.

The latitudinal variations of the amplitude of the harmonic signal suggests that multidecadal oscillations, such as AMO, are essentially controlled by the northern regions of the North Atlantic ocean where deep water formation is favored, and thus control the THC time variability. The results of Figure 11 are in accord with the spatial

pattern of AMO resulting from EOF analysis of Parker et al. (2007) (see their fig. 6) and with the hypothesis of Frankcombe et al (2010) of the Arctic origin of the AMO pattern.

## 5. Correlation of SST with NAOI

The simultaneous occurrence of a cycle of about 70 years both in the North Atlantic and the Mediterranean poses the problem of whether or not a single source of this periodicity exists. Schlesinger and Ramankutty (1994), who observed a similar cycle in the atmospheric near surface temperature of the North Atlantic and its bounding Northern Hemisphere continents, suggested three possible sources: an external oscillatory forcing, such as by a variation in the solar constant; a random forcing, such as by white noise; an internal oscillation of the atmosphere-ocean system. They argued that, due to the uneven spatial distribution of the oscillation the first two must be excluded because the first should have produced a global response and this did not happen as demonstrated by Schlesinger and Ramankutty (1994); the second, the white noise forcing, should have produced an ocean-wide response with some kind of signature also in the SST field and this did not happen as demonstrated by our analysis.

The above arguments suggest that the most probable cause of the North Atlantic and Mediterranean oscillations could be an internal oscillation of the atmospheric-ocean system. If this is true we should be able to find some kind of correlation between long term SST variations and some key climatic index, representative of the coupled ocean-atmosphere system in the North Hemisphere. NAO is one of these indices.

Actually there are a variety of NAO indices available from several climate centres and various authors. Most of them are derived either from sea level pressure anomaly

differences between two stations or from the principal components time series of the leading EOF of the sea level pressure.

The station-based NAO indices have the advantage of going back to the mid-19th century even if, due to the movement of the NAO centres through the year, they are able to capture the NAO variability for a part of the year only. Figure 12 reports Winter NAO indices provided by three different sources: UCAR NAO (Hurrell, 1995), Climate Research Unit (CRU) (Hurrell 1995; Jones et al., 1997) and NAOI (Li and Wang, 2003). The three indices show many similarities and some differences. More specifically, for frequencies around 10 years or higher there is a complete correspondence between the three series while lower frequencies have different amplitudes. In particular, the NAOI exhibits a higher amplitude multi-decadal oscillation that vaguely resemble the AMO one.

Li and Wang (2003) defined their NAO Index (NAOI) as the difference in the normalized sea level pressure (SLP) regionally zonal-averaged over the North Atlantic sector from 80° W to 30° E between 35° N and 65° N. They demonstrated that NAOI is able to describe well the large-scale circulation features of NAO and suggested that this index can be used to characterize the NAO for all seasons. The following analysis is based on NAOI.

The correlation between NAOI and SST was computed for each grid point over the North Atlantic and Mediterranean Sea for each season and year using HadISST (fig.13). In Figure 13 the SST and NAOI correlation pattern shows the typical tripole structure (Cayan et al., 1992; Sutton et al., 2000) with alternate significantly anti-correlated in the sub-polar region and in the tropical Atlantic ocean and positive correlation in between.

This corresponds to the typical SST pattern that accompanies the positive (negative) NAO regime with low (high) temperatures in the higher latitude regions and south of 20 °N, and higher (lower) SSTs between 25 °N and 45° N (Flatau et al. 2003). A significant negative correlation is also observed in the Eastern Mediterranean Sea, but only in winter, while few grid points passed the test in the western Mediterranean Sea and the Adriatic Sea during Autumn. Similar results are obtained using ERSST with relatively smoother maps (not shown). The only remarkable difference has been observed in Autumn when the northern pole of the correlation maps do not passed the 90% confidence level test.

On the basis of these results we focused our analysis on the Winter (JFM) correlation between NAOI and SST in the subpolar gyre (SPG), in the subtropical gyre (STG) and the Mediterranean Sea. The SPG and the STG SST's have been computed by averaging the SST in all the grid points within the Northern and Southern centers of the Atlantic Tripole respectively. Figure 14 is based on the HadISST time series and shows the time variability of the winter SST in the three selected areas together with the AMO and the NAOI (note that the NAOI has been plotted with the sign changed to facilitate the interpretation). Similar calculations made considering the half cold part of the year (DJFMA) rather than JFM give very nearly identical results (not shown).

As expected the NAOI correlates (negatively) quite well with the three time series and with AMO for most of the period under investigation. All the relative minima and maxima of the SPG SST series correspond to equivalent NAOI peaks (with the exception of the 1925 NAOI peak) even though, after 1940, NAOI seems to lead SPG SST by 1-2

years. Either NAOI and AMO or any of the three SSTs show evidence of a multi-decadal oscillation with period of about half of the length of the time series.

At annual scale similar correlations also exist, as qualitatively suggested by the autocorrelation analysis of the global SST time series (fig. 10). A quantitative measure of the functional coupling between Mediterranean Sea SST and other North Atlantic time series is the estimate of the magnitude squared coherence (MSC). The MSC is a normalized cross-spectral density function, and measures the strength of association and relative linearity between stationary processes on a scale from 0 to 1 (Wang et al., 2004). Given two functions  $x(t)$  and  $y(t)$  the MSC is defined as:

$$\gamma_{xy}^2(f) = \frac{|P_{xy}(f)|^2}{P_{xx}(f)P_{yy}(f)}$$

where  $P_{xy}(f)$  is the complex cross-spectral density, and  $P_{xx}(f)$  and  $P_{yy}(f)$  are the auto-spectral densities at frequency  $f$ . The confidence limit of the estimated coherence at a given level  $\alpha$  (95% is  $\alpha=0.05$ ) has been calculated as  $1 - \alpha^{1/(K-1)}$ , where  $K$  is the number of tapers used for the MTM.

The MSC between the Mediterranean SST time series and each other time series of the North Atlantic Ocean: NAOI, AMO, Sub Polar Gyre region SST and Subtropical Gyre region SST is shown in figure 15. The four Atlantic indices are significantly coherent with the Mediterranean SST time series at low frequencies corresponding to multidecadal periods with confidence limit between 95% and 99% or more. All the Atlantic indices are significantly coherent with the Mediterranean time series (confidence limit 90%) for periods longer than about 40 yr. Moreover second coherence pick around

18 yr is present. Other higher frequency peaks exceeding the 95% confidence limit are also observed for coherences between Mediterranean SST and the Atlantic indices.

## 6. Conclusion and discussion

In this paper we analyzed the most extensive SST datasets for Mediterranean Sea currently available, from 1854 to 2009, and looked for connections with the SST of the global ocean, and in particular of the North Atlantic.

We first evaluated the robustness and reliability of the two reconstructed SST datasets (HadISST and ERSST.v3) over the Mediterranean Sea, finding that damping or other potential distortions due to interpolation are not dominant when yearly averages are used.

Switching to monthly means, larger differences between the two interpolated data sets have been found, that exhibit a marked annual cycle, more pronounced prior to 1941 when different SST bias adjustments were applied.

The same annual cycle was found comparing the three analyzed datasets (HadISST, ERSST.v3 and ICOADS 2.5) with recent satellite estimate for the period 1985-2005 validated against in situ observations. We concluded that the three time series are interchangeable when averaged over the year, and can be used to evaluate the long term variability of the SST field also at the Mediterranean regional scale. Monthly time series should be used with more care.

Following the guidelines proposed by Ghil et al. (2002), we have applied the Multi Taper Method (MTM) and the SSA analysis to the de-trended yearly SST derived from the ERSST.v3 dataset, to investigate the low frequency variability of the Mediterranean Sea. We found 6 peaks at the 99% confidence level and 5 more peaks at the 95% confidence



level. However, the peaks over the 99% confidence limit, corresponding to 7.3, 4.3 and 3.2 years, are associated with very weak power in the spectrum (fig. 9b), while those at 73, 6.3, and 2.8 years correspond to significant spectral bands. Some of these peaks qualify as harmonics in the reshaping procedure: 6.3 and 2.8 years, and two high frequency peaks at 3.9 and 2.2 years that are close to the 95% confidence limit. We noted that the higher frequency peaks are linked to the scale of variability of the ENSO's quasi-biennial and low-frequency modes (Rasmusson et al, 1990; Jiang et al, 1995; Yiou et al, 2000). The lower frequency band that peaks at 73 years (very close to the AMO period), does not pass the reshaping test. Our spectral analysis suggests that the four higher frequency peaks are likely to contain a harmonic phase-coherent oscillation with, at least, a 90% level of confidence, but the same is not true for the low frequency band at 73 years where the reshaped and the unreshaped spectra are identical. However, from the overall results of the MTM and SSA spectral analysis and from the physical correspondence of the multidecadal oscillation with some geophysical phenomenon, is a matter of fact that the multidecadal band, corresponding to the 73 years line, is a significant feature of the spectrum.

The analysis of the SST field over Atlantic Ocean confirm the importance of a similar multidecadal oscillation with a maximum at sub-polar latitudes (fig. 11). This result is agreement with the spatial pattern of AMO resulting Parker et al. (2007) and with the hypothesis of Frankcombe et al (2010) of the Arctic origin of the AMO pattern.

A quantitative measure of the functional coupling between Mediterranean Sea SST and other North Atlantic time series has been confirmed by magnitude squared

coherence analysis (fig. 15) where Mediterranean SST is high coherent with the Atlantic indices for period longer than about 40 years.

Since the Mediterranean and North Atlantic oscillation are coherent at multidecadal scale, one should wonder about the existence of physical mechanisms that connect the two areas. Dima and Lohmann (2007) have recently proposed for AMO a deterministic mechanism based on atmosphere-ocean-ice interaction, synthesized in Fig. 8 of their paper, that relates the multidecadal SST variability to the THC strengthening. They argued that the atmospheric response to the positive SST anomalies in the North Atlantic is represented by a SLP low over the SSTs pattern including Eurasia region and therefore the Mediterranean Region. Afterwards, the effect is transferred in the North Pacific through atmospheric teleconnections producing a SLP high, that determines a maximum pressure gradient over Fram Strait, increasing Arctic sea ice and freshwater export with a consequent THC reduction. This sequence is cyclically repeated producing the 70 years multi-decadal oscillation.

The results of our data analysis, that identify the maximum of the 70 years multidecadal signal at the subpolar latitudes (fig. 11), is consistent with this schema. However the presence of a similar oscillation over the Mediterranean Sea is out of the Dima and Lohmann schema. Nevertheless, several authors have suggested that the Mediterranean outflow of saltier waters throughout Gibraltar strait can play a role in the modulation of the North Atlantic THC (Artale et al., 2006; Calmanti et al., 2006; Lozier and Stewart, 2008). However, the impact of the Mediterranean Outflow Water (MOW), an intermediate saltier water that outflows from the Gibraltar strait into the Atlantic Ocean, on the strength of the Atlantic THC is considered relatively small (e.g.,

Rahmstorf, 1998), even though Artale et al. (2002) and Calmanti et al. (2006) suggested that this water can contribute to the strengthening and variability of the North Atlantic THC. Moreover Lozier and Stewart (2008) in an analysis of historical hydrographic data in the eastern North Atlantic suggest a connection between the northward penetration of the MOW and the location of the subpolar front, leaving open the discussion of the possible effect of water mass transformation in the subpolar regions.

In a revised version of Dima et al. (2007) schema, where the Mediterranean sea is included, the North Atlantic-Mediterranean-Arctic Sea can be considered as an unique oceanographic system, where the physical processes within the straits that connect the three sub-systems play an important role in determining the freshwater and salt water exchange between marginal seas and open ocean (Sannino et al., 2009). The role of the MOW in modulating the THC has not yet proved even if it should be important in modulating surface heat fluxes in the deep water formation region of the north Atlantic (Wu et al., 2007) by advecting salty water of Mediterranean origin.

Recently Frankcombe et al. (2010), proposed that the multi-decadal variability of the North Atlantic is dominated by two main time scale (20–30 and 50–70 yr) . The first has an ocean internal origin caused by the variability of the Atlantic Meridional Overturning Circulation, while the 50-70 year variability is related to atmospheric forcing and exchange process between Atlantic and Arctic Ocean. Under this new scheme the hypothesis of an atmospheric origin also for the Mediterranean 70 years signal is reinforced also taking into account the absence of lag between the AMO and Mediterranean index.

Our analysis of the Mediterranean SST variability does not allow to definitive answer to the question whether the forcing of the observed multi-decadal signal has an atmospheric origin or there is some contribution due to the Mediterranean THC. Coupled ocean-atmosphere models could contribute to investigate the origin of the Mediterranean Multidecadal Oscillation and to separate the concurring contributions of the atmosphere and the Mediterranean thermohaline circulation. However, given the importance of the water masses exchanges throughout the strait of Gibraltar, it is very important to include explicitly the strait in the coupled model with a physical connection between the Mediterranean Sea and the Atlantic Ocean. In HadCM3 Mediterranean water is partially mixed with Atlantic water across the Strait of Gibraltar as a simple representation of water mass exchange since the channel is not resolved in the model. This can partially limit the results of the investigation on the Mediterranean multidecadal fluctuations. Sannino et al. (2009), using eddy permitting Mediterranean model with a two-way grid refinement in the region of the Strait of Gibraltar, have demonstrated how a more realistic description of the strait can influence the characteristics of the inflowing Modified Atlantic Water and Mediterranean outflow in terms of thickness and depth profiles. These differences propagate into the whole basin, have an impact on the water column stratification, and consequently on the characteristics of the convection events and, in turn, on the variability of the Mediterranean THC. The results of Sannino et al. (2009) clearly indicate the importance of explicitly include the Gibraltar connection also in coupled atmosphere-ocean models to investigate multidecadal fluctuation in the Mediterranean Sea and to correctly separate atmosphere and internal ocean contribution to such oscillations.

*Acknowledgments.*

First of all we wish to thank the three anonymous referees for the critical review of the manuscript and for the helpful suggestions.

ERSST.v3 data provided by NOAA satellite and Information Service - National Environmental, Satellite and information Service (NESDIS).

(<http://lwf.ncdc.noaa.gov/oa/climate/research/sst/ersstv3.php>).

HadISST data provided by UK Meteorological Office, Hadley Centre. HadISST 1.1 - Global sea-Ice coverage and SST (1870-Present). British Atmospheric Data Centre, 2006, Date of citation,. Available from <http://badc.nerc.ac.uk/data/hadisst/>. ICOADS data provided by the NOAA/OAR/ESRL PSD, Boulder, Colorado, USA, from their Web site at <http://www.esrl.noaa.gov/psd/>. We thank Dr. Tom Smith for providing global bias adjustment data for prior 1941 SSTs and Drs Rober Evans, Viva Banzon and Roberto Iacono for stimulating discussions.

## References

Artale V., S. Calmanti and A. Sutera, 2002: North Atlantic THC sensitivity to Mediterranean waters, *Tellus, Series A*, Vol.54, Issue 2, 159-174.

Artale, V. et al., 2006: The Atlantic and Mediterranean Sea as connected systems. In: P. Lionello, P., Malanotte-Rizzoli & R. Boscolo (Eds), *Mediterranean Climate Variability*, Amsterdam: Elsevier, pp. 283-323

Bottomley, M., C. K. Folland, J. Hsiung, R. E. Newell, and D. E. Parker, 1990: Global Ocean Surface Temperature Atlas. Her Majesty's Stationery Office, Norwich, United Kingdom, 24 pp. + 313 color plates.

Broomhead, D. S., and G. P. King, 1986: Extracting qualitative dynamics from experimental data, *Phys. D*, 20, 217–236.

Calmanti S., Artale V and A. Sutera, 2006: North Atlantic MOC variability and the Mediterranean outflow: a box-model study; *Tellus, Series A* , 58A, 416-423.

Delworth, T. L. and Mann, M. E., 2000: Observed and simulated multidecadal variability in the Northern Hemisphere. *Clim. Dyn.*, 16, 661– 676.

Dijkstra, H. A., and M. Ghil, 2005: Low-frequency variability of the large-scale ocean circulation: A dynamical systems approach, *Rev. Geophys.*, 43, RG3002, doi:10.1029/2002RG000122.

Dima M. and G. Lohmann, 2007: A Hemispheric Mechanism for the Atlantic Multidecadal Oscillation. *Journal of Climate*, 20, 2706-2719.

Dong, B., and R.T. Sutton, 2005: Mechanism of Interdecadal Thermohaline Circulation Variability in a Coupled Ocean–Atmosphere GCM. *J. Climate*, 18, 1117–1135.

Enfield, D. B., A. M. Mestas Nuñez, and P. J. Trimble, 2001: The Atlantic Multidecadal Oscillation and its relation to rainfall and river flows in the continental U.S., *Geophys. Res. Lett.*, 28(10), 2077–2080.

Flatau M. K., L. Talley, P.P Niiler, 2003: The North Atlantic Oscillation, Surface Velocities, and SST Changes in the Subpolar North Atlantic. *Journal of Climate*, Vol. 16, 2355-2369.

Folland, C. K., and D. E. Parker, 1995: Correction of instrumental biases in historical sea surface temperature data. *Quart. J. Roy. Meteor. Soc.*, 121, 319–367.

Fraedrich, K., 1986: Estimating the dimension of weather and climate attractors, *J. Atmos. Sci.*, 43, 419–432.

Frankcombe, L. M., A. von der Heydt, and H. A. Dijkstra, 2010: North Atlantic Multidecadal Climate Variability: An Investigation of Dominant Time Scales and Processes. *Journal of Climate*, 23, 3626-3638.

Ghil M., M. R. Allen, M. D. Dettinger, K. Ide, D. Kondrashov, M. E. Mann, A. W. Robertson, A. Saunders, Y. Tian, F. Varadi, and P. Yiou, 2002: Advanced Spectral Methods For Climatic Time Series, *Reviews of Geophysics*, 40, 1, 1003, doi:10.1029/2000RG000092.

Grist J. P., R. Marsh, S. A. Josey, 2009: On the Relationship between the North Atlantic Meridional Overturning Circulation and the Surface-Forced Overturning Streamfunction. *Journal of Climate*, Vol. 22, 4989-5002.

Grosfeld K. , G. Lohmann and N. Rimbu, 2008: The impact of Atlantic and Pacific Ocean sea surface temperature anomalies on the North Atlantic multidecadal variability, *Tellus* , 60A, 728–741.

Hodson, D.L.R., R.T. Sutton, C. Cassou, N. Keenlyside, Y. Okumura, and T. Zhou, 2009: Climate impacts of recent multidecadal changes in Atlantic Ocean Sea Surface Temperature: a multimodel comparison. *Clim. Dyn.* doi:10.1007/s00382-009-0571-2



Huck, T., A. Colin de Verdière, and A. J. Weaver, 1999: Interdecadal variability of the thermohaline circulation in box-ocean models forced by fixed surface fluxes. *J.Phys. Oceanogr.*, 29, 865–892.

Hurrell, J.W., 1995: Decadal Trends in the North Atlantic Oscillation: Regional Temperatures and Precipitation. *Science*: Vol. 269, pp.676-679.

Jiang, N., D. Neelin, M. Ghil, 1995: Quasi-quadrennial and quasi-biennial variability in the equatorial Pacific, *Clim. Dyn.* 12, 101–112.

Jones P. D., T. Jonsson and D. Wheeler, 1997: Extension To The North Atlantic Oscillation Using Early Instrumental Pressure Observations From Gibraltar And South-West Iceland, *International Journal of Climatology*, Vol. 17, 1433-1450.

Jungclaus, J.H., H. Haak, M. Latif, and U. Mikolajewicz, 2005: Arctic–North Atlantic Interactions and Multidecadal Variability of the Meridional Overturning Circulation. *Journal of Climate*, 18, 4013–4031.

Knight, J. R., R. J. Allan, C. K. Folland, M. Vellinga, and M. E. Mann ,2005: A signature of persistent natural thermohaline circulation cycles in observed climate, *Geophys. Res. Lett.*, 32, L20708, doi:10.1029/ 2005GL024233.

Knight, J. R., C. K. Folland, and A. A. Scaife, 2006: Climate impacts of the Atlantic Multidecadal Oscillation, *Geophys. Res. Lett.*, 33, L17706, doi:10.1029/2006GL026242.

Lees, . M., J. Park, 1995: Multiple-Taper Spectral Analysis: A stand-alone C-Subroutine, *Computer and Geoscience*, Vol.1, N0. 2, pp. 199-236

Li, J. and J. X. L. Wang, 2003: A New North Atlantic Oscillation Index and Its Variability, *Advances in Atmospheric Sciences*, vol. 20, no. 5, 2003, pp. 661–676.

Lozier M. S. and N. M. Stewart, 2008: On the Temporally Varying Northward Penetration of Mediterranean Overflow Water and Eastward Penetration of Labrador Sea Water, *Journal of Physical Oceanography*, Vol. 38, 2097-2103.

Marullo S. , B. Buongiorno Nardelli, M. Guarracino, and R. Santoleri, 2007: Observing the Mediterranean Sea from space: 21 years of Pathfinder-AVHRR sea surface temperatures (1985 to 2005): re-analysis and validation. *Ocean Sci.*, 3, 299–310.

Mohino, E., S. Janicot and J. Bader (2010), Sahel rainfall and decadal to multi-decadal sea surface temperature variability, *Clim. Dyn.* DOI: 10.1007/s00382-010-0867-2

Parker, D., C. Folland, A. Scaife, J. Knight, A. Colman, P. Baines, and B. Dong, 2007: Decadal to multidecadal variability and the climate change background, *J. Geophys. Res.*, 112, D18115, doi:10.1029/2007JD008411

Pisacane G., V. Artale, S. Calmanti and V. Rupolo, 2006: Decadal Oscillations in the Mediterranean Sea: A Result of the Overturning Circulation Variability in the Eastern Basin? *Climate Research*, Vol. 31, N. 2-3, July 27.

Rahmstorf, S., 1998: Influence of Mediterranean outflow on climate. *Eos*, 79 (24), 281-282.

Rasmusson, E.M., X. Wang, C.F. Ropelewski, 1990: The biennial component of ENSO variability, *J. Mar. Syst.*, 1, 71–96.

Rayner, N. A.; Parker, D. E.; Horton, E. B.; Folland, C. K.; Alexander, L. V.; Rowell, D. P.; Kent, E. C.; Kaplan, A., 2003: Global analyses of sea surface temperature, sea ice, and night marine air temperature since the late nineteenth century, *J. Geophys. Res.*, Vol. 108, No. D14, 4407 10.1029/2002JD002670

Rayner N. A., P. Brohan, D. E. Parker, C. K. Folland, J. J. Kennedy, M. Vanicek, T. J. Ansell, And S. F. B. Tett, 2006: Improved Analyses of Changes and Uncertainties in Sea Surface Temperature Measured In Situ since the Mid-Nineteenth Century: The HadSST2 Dataset, *Journal of Climate*, Vol 19, 446-469.

Reid J. L., 1979: On the Contribution of the Mediterranean Sea outflow to the Norwegian-Greenland Sea. *Deep-Sea Research*, Vol. 26, 1199-1223.

Reynolds, R. W., T. M. Smith, C. Liu, D. B. Chelton, K. S. Casey, and M. G. Schlax, 2007: Daily high-resolution blended analyses for sea surface temperature. *J. Climate*, 20, 5473-5496.

Sannino, G., L. Pratt, and A. Carillo, 2009: Hydraulic Criticality of the Exchange Flow through the Strait of Gibraltar. *J. Phys. Oceanogr.*, 39, 2779–2799.

Sannino G., M. Herrmann , A. Carillo, V. Rupolo, V. Ruggiero, V. Artale, P. Heimbach, 2009: An eddy-permitting model of the Mediterranean Sea with a two-way grid refinement at the Strait of Gibraltar. *Ocean Modelling*, 30, 56-73, doi:10.1016/j.ocemod.2009.06.002

Schlesinger, M. E. and N. Ramankutty, 1994: An Oscillation in the global climate system of period 65-70 years, *Nature*, Vol. 367, 723-726. doi:10.1038/367723a0;

Slepian, S., 1978: Prolate spheroidal wave functions, Fourier analysis and uncertainty, V, The discrete case, *Bell. Syst. Tech. J.*, 57, 1371–1430.

Smith, T. M., and R. W. Reynolds, 2002: Bias corrections for historic sea surface temperatures based on marine air temperatures. *J. Climate*, 15, 73–87.

Smith, T.M., and R.W. Reynolds, 2003: Extended Reconstruction of Global Sea Surface Temperatures Based on COADS Data (1854-1997). *Journal of Climate*, 16, 1495-1510.

Smith, T.M., and R.W. Reynolds, 2004: Improved Extended Reconstruction of SST (1854-1997). *Journal of Climate*, 17, 2466-2477.

Smith, T.M., R.W. Reynolds, Thomas C. Peterson, and Jay Lawrimore, 2008: Improvements to NOAA's Historical Merged Land-Ocean Surface Temperature Analysis (1880-2006) *Journal of Climate*, 21, 2283-2296.

Sutton R. T., and D.L.R. Hodson, 2005: Atlantic ocean forcing of North America and European Summer Climate. *Science* Vol. 309, No. 5731, pp. 115-118;

te Raa L. A. and H. A. Dijkstra, 2002: Instability of the Thermohaline Ocean Circulation on Interdecadal Timescales, *Journal of Physical Oceanography*, Vol. 32, 138-160.

Thomson, D. J., 1982: Spectrum estimation and harmonic analysis, *Proc. IEEE*, 70, 1055–1096.

Thompson D.W.J., J.J. Kennedy, J.M. Wallace, and P.D. Jones 2008: A large discontinuity in the mid-twentieth century in observed global-mean surface temperature. *Nature*, 453, 646-649 doi:10.1038/nature06982.

Trenberth, K. E., and D. J. Shea (2006), Atlantic hurricanes and natural variability in 2005, *Geophys. Res. Lett.*, 33, L12704, doi:10.1029/2006GL026894.

Trenberth, K.E., P.D. Jones, P. Ambenje, R. Bojariu, D. Easterling, A. Klein Tank, D. Parker, F. Rahimzadeh, J.A. Renwick, M. Rusticucci, B. Soden and P. Zhai, 2007: Observations: Surface and Atmospheric Climate Change. In: *Climate Change 2007: The Physical Science Basis. Contribution of Working Group I to the Fourth Assessment Report of the Intergovernmental Panel on Climate Change* [Solomon, S., D. Qin, M. Manning, Z. Chen, M. Marquis, K.B. Averyt, M. Tignor and H.L. Miller (eds.)]. Cambridge University Press, Cambridge, United Kingdom and New York, NY, USA.

UK Meteorological Office, Hadley Centre. HadCM3 Control Run Model Data, [Internet]. British Atmospheric Data Centre, 2006-, *Date of citation*. Available from <http://badc.nerc.ac.uk/data/hadcm3-control>.

Van den Dool, H. M., S. Saha, and A. Johansson, 2000: Empirical orthogonal teleconnections. *J. Climate*, **13**, 1421–1435.

Vautard, R., and M. Ghil, 1989: Singular spectrum analysis in nonlinear dynamics, with applications to paleoclimatic time series, *Phys. D*, 35, 395–424.

Vautard, R., P. Yiou and M. Ghil, 1992: Singular-spectrum analysis: A toolkit for short, noisy chaotic signals, *Physica* 58D, 95-126.

Vellinga, M., and P. Wu, 2004: Low-latitude freshwater influence on centennial variability of the Atlantic thermohaline circulation. *J. Climate*, 17, 4498–4511.

Wang S.Y., X. Liu , J. Yianni, R. C. Miall, T. Z. Aziz, J. F. Stein, 2004: Optimising coherence estimation to assess the functional correlation of tremor-related activity between the subthalamic nucleus and the forearm muscles. *J. of Neuroscience Methods*, 136 (2004) 197–205

Wittenberg A. T., Are historical records sufficient to constrain ENSO simulations?, 2009: *Geophysical Research Letters*, Vol. 36, L12702, doi:10.1029/2009GL038710

Worley S. J., S. D. Woodruff, R. W. Reynolds, J. S. Lubker, N. Lott, 2005: Icoads release 2.1 data and products, *int. j. climatol.* 25: 823–842, doi: 10.1002/joc.1166.

Wu W., G. Danabasoglu, and W.G., 2007: Large, On the effects of parameterized Mediterranean overflow on North Atlantic ocean circulation and climate, *Ocean Modelling*, Volume 19, Issue 1-2, Pages 31-52.

Yiou, P., D. Sornette, and M. Ghil, 2000: Data-adaptive wavelets and multi-scale SSA, *Phys. D*, 142, 254–290.

## List of Figures

Fig. 1. Percentage of grid boxes with monthly ICOADS SST data in the Mediterranean Sea.

Fig. 2. Percentage of Mediterranean grid boxes where yearly SST averages were computed (12 monthly SST available). In years falling below the horizontal dotted line (15%), spatial averages of the Mediterranean Sea surface temperature were not computed.

Fig. 3. Mediterranean annual SST anomaly (respect to the 1971-2000 average) from 1854 to 2008. Red line ERSST.v3, blue line HadISST, green line ICOADS 2.5. The black solid line represents the filtered average of the three datasets.

Fig. 4. Monthly differences SST anomalies in the Mediterranean Sea (respect to the 1971-2000 average). a) ERSST.v3 - HadISST; b) ERSST.v3 - ICOADS 2.5; c) HadISST - ICOADS 2.5.

Fig. 5. Monthly differences between reconstructed SST anomalies and Reynolds OIv2 (a) or Pathfinder OISST (b) in the Mediterranean Sea (anomalies respect to the 1971-2000 average). (c) Differences between in situ and satellite SSTs. Red crosses are CTD - OiPath, Black crosses are XBT - OiPath. The solid line indicates the difference between in situ SST (XBT + CTD) and OiPath.



Fig. 6. Mean monthly bias of ERSST and HadISST reconstruction respect to in situ observations.

Fig. 7 Autocorrelation coefficients for different time lags of the Mediterranean using HadISST (red triangles) and ERSST (black squares).

Fig. 8. a) Singular spectrum of SST time series, the eigenvalues are plotted in decreasing order, the embedding dimension is  $M=70$ , which represents a time window of 70 years, b) First two empirical orthogonal functions (EOFs) of the Mediterranean SST time series c) time evolution of the mean annual SST of the Mediterranean Sea from 1854 to 2008 (black thin line) and the reconstructed time series (black thick line) are shown, the latter is based on SSA with a 70-year window, which retains the first two modes.

Fig. 9. Comparison between MTM spectra obtained by harmonic analysis test and adaptively weighted estimation against red noise background for the ERSST.v3 series of the Mediterranean Sea. Shown are (a) harmonic signal (variance ratio) F test with median, 90%, 95%, and 99% significance levels indicated and (b) reshaped (orange) versus unreshaped (black) adaptively weighted MTM spectrum based on  $p=2$  and  $K=3$ , and a 90% F test significance criterion for reshaping.

Fig. 10. Autocorrelation coefficients for different world ocean regions (based on HadISST data set). Units for abscissas are years.

Fig. 11. Latitudinal variation of the amplitude of the harmonic signal in the North Atlantic (based on ERSSTV3 data). Symbols indicate the frequency where lines peak.

Fig. 12. Winter (JFM) NAO Index from different sources. (a) Climate Analysis Section of NCAR (Hurrell, 1995), (b) CRU-UEA, (c) Li and Wang (2003). The thin lines refer to yearly values while the thick lines refer to a 7 years gaussian smoothing of the yearly values.

Fig. 13. Correlation maps between HadISST and NAOI. The thick contour line represents the -0.4 correlation level. Intervals between contour lines is 0.05. Colored regions represent areas where the 90% confidence level test has passed.

Fig. 14 Winter SST anomaly in the Subpolar Gyre (SPG red solid line), in the subtropical gyre (STG yellow solid line) and in the Mediterranean Sea (Blue solid line) and AMO (green solid line). The dotted line represents the NAOI index (black). All the anomalies were calculated with respect to the mean of the entire period plotted in the figure using HadISST. NAOI has been plotted with the sign changed in order to better show the correlations with SSTs. All the time series have been filtered using a 7 year Gaussian filter. The center of the SPG and STG areas are defined as grid point where correlation is less of equal -0.4 (thick line in figure 13).

Fig. 15. Magnitude Squared Coherence estimation between Mediterranean SST and NAO (a), Mediterranean SST and AMO(b), Mediterranean SST and Sub Polar Gyre SST (c), Mediterranean SST and Sub Polar Gyre SST (d). Green , blue and yellow lines represent the 90%, 95% and 99% confidence limit respectively.

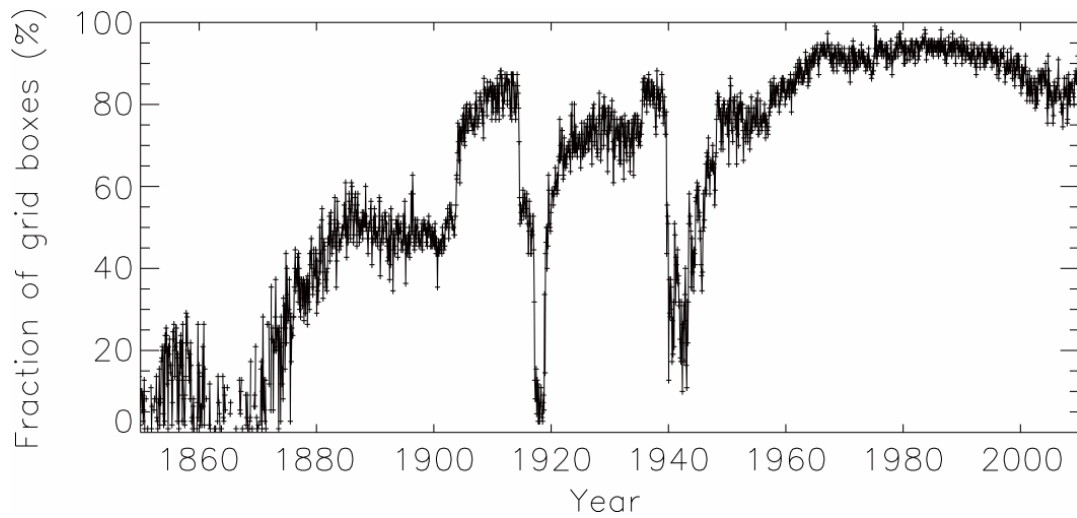


Fig. 1. Percentage of grid boxes with monthly ICOADS SST data in the Mediterranean Sea.

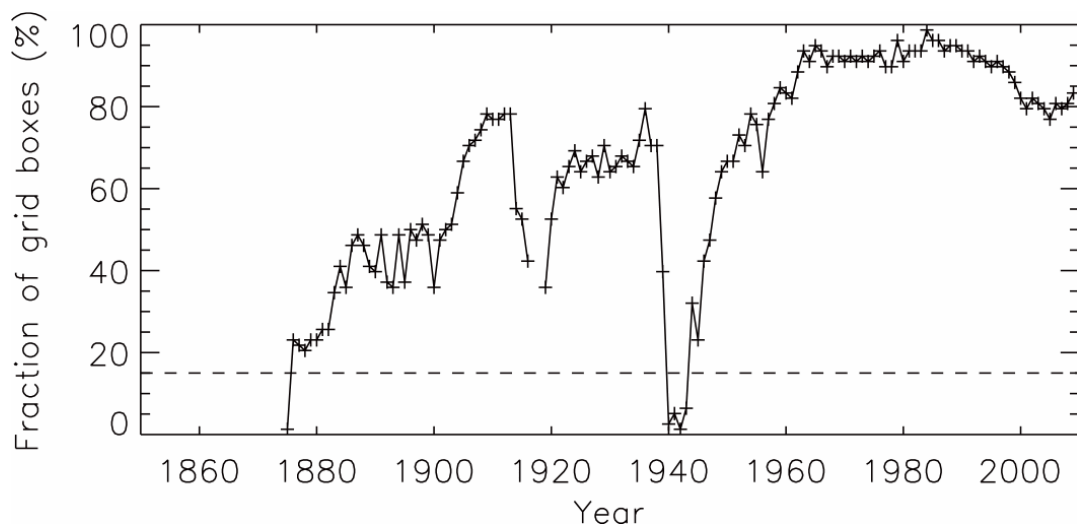


Fig. 2. Percentage of Mediterranean grid boxes where yearly SST averages were computed (12 monthly SST available). In years falling below the horizontal dotted line (15%), spatial averages of the Mediterranean Sea surface temperature were not computed.

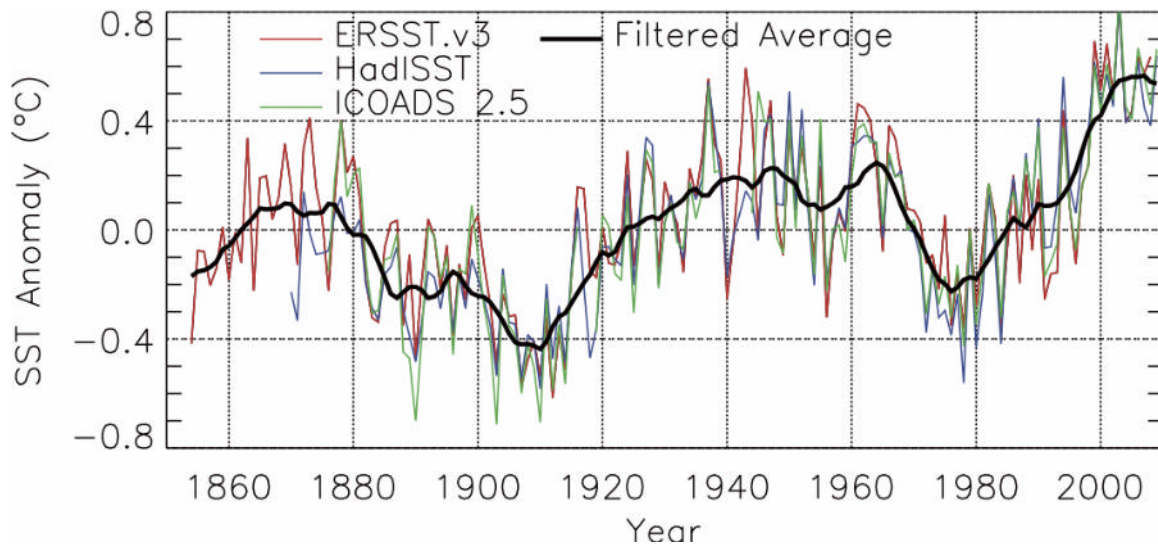


Fig. 3. Mediterranean annual SST anomaly (respect to the 1971-2000 average) from 1854 to 2008. Red line ERSST.v3, blue line HadISST, green line ICOADS 2.5. The black solid line represents the filtered average of the three datasets.

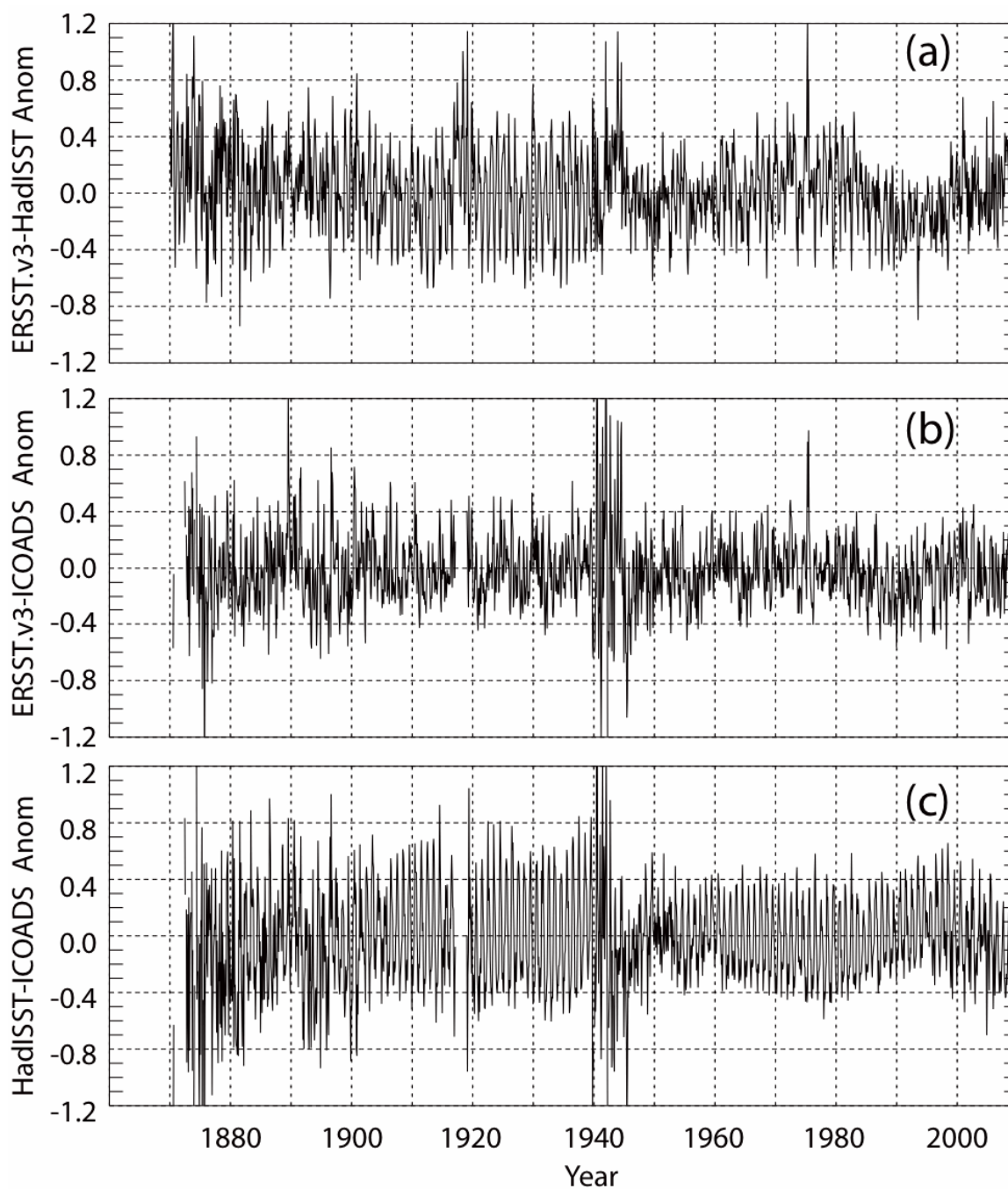


Fig. 4. Monthly differences SST anomalies in the Mediterranean Sea (respect to the 1971-2000 average). a) ERSST.v3 - HadISST; b) ERSST.v3 - ICOADS 2.5; c) HadISST - ICOADS 2.5.

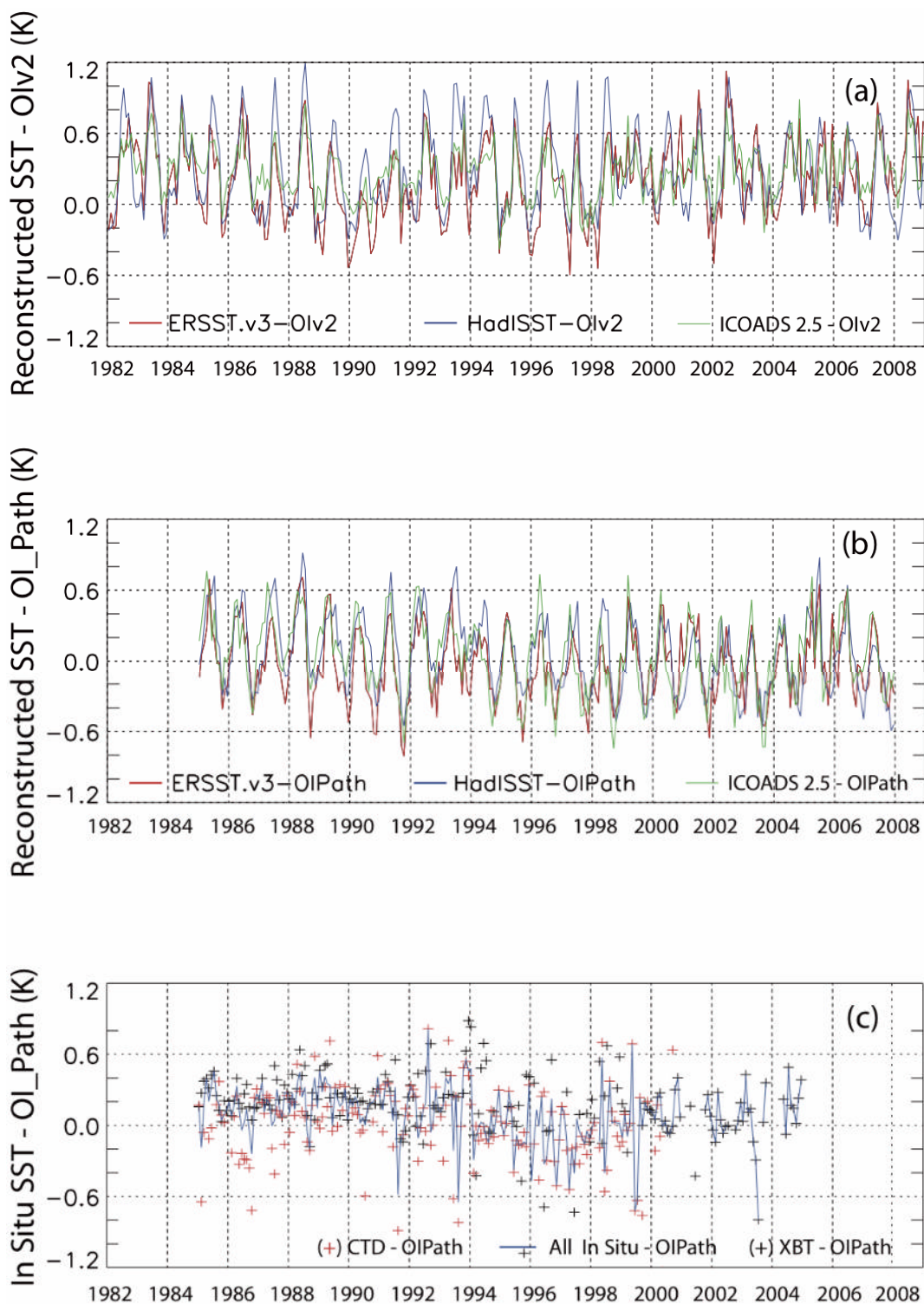


Fig. 5. Monthly differences between reconstructed SST anomalies and Reynolds OIv2 (a) or Pathfinder OISST (b) in the Mediterranean Sea (anomalies respect to the 1971-2000

average). (c) Differences between in situ and satellite SSTs. Red crosses are CTD - OIPath, Black crosses are XBT - OiPath. The solid line indicates the difference between in situ SST (XBT + CTD) and OiPath.

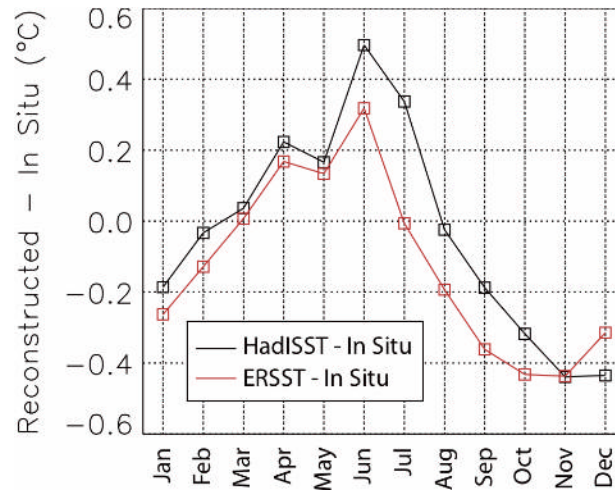


Fig. 6. Mean monthly bias of ERSST and HadISST reconstruction respect to in situ observations.



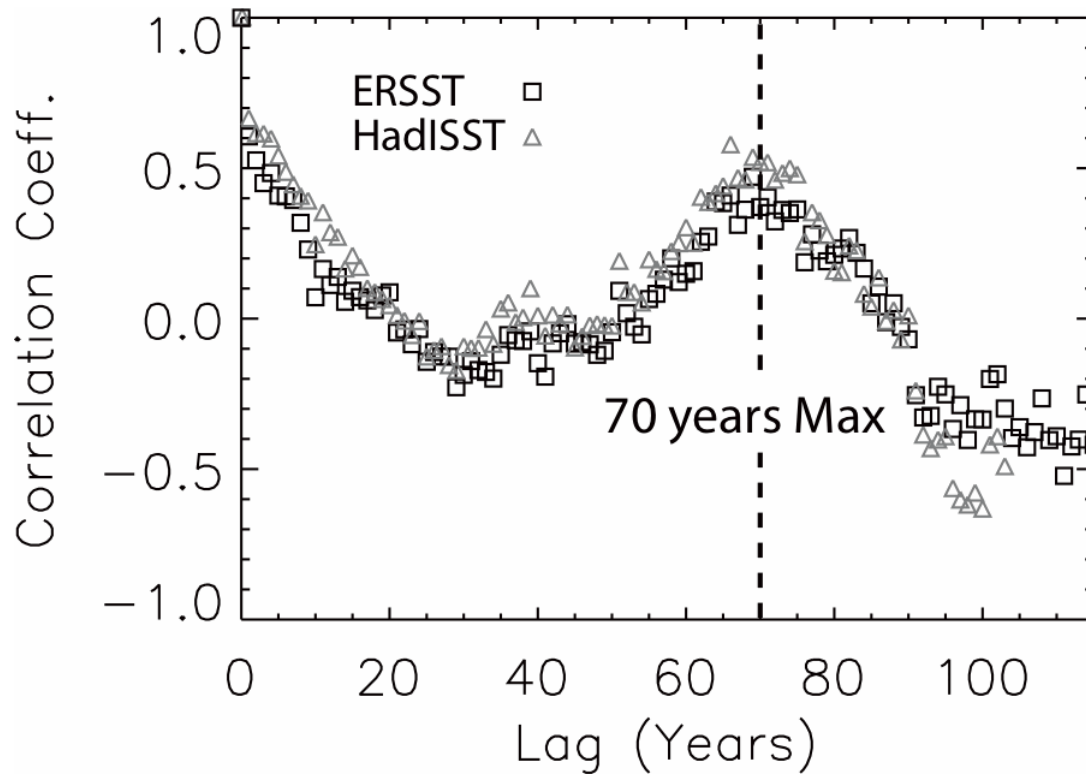


Fig. 7. Autocorrelation coefficients for different time lags of the Mediterranean using HadISST (red triangles) and ERSST (black squares).

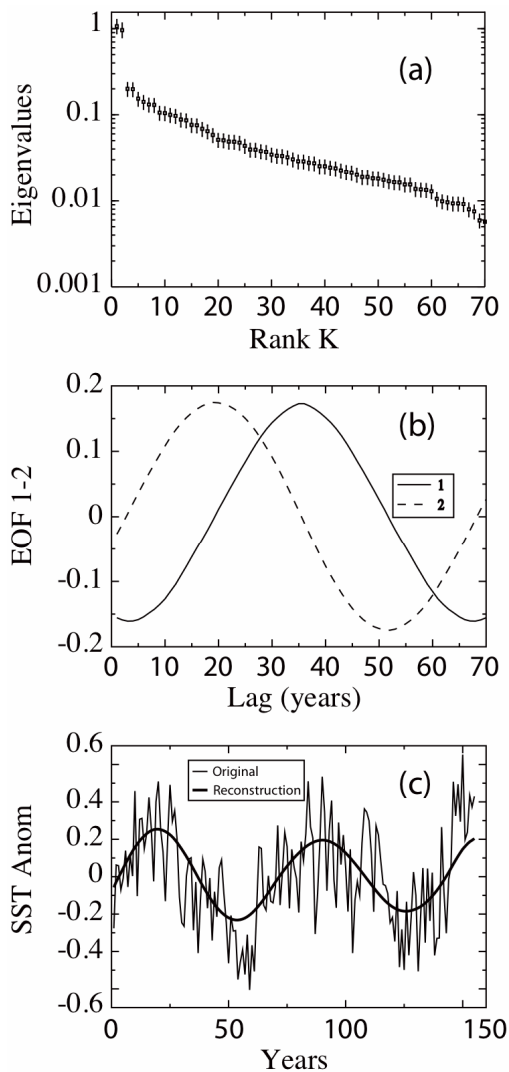


Fig. 8. a) Singular spectrum of SST time series, the eigenvalues are plotted in decreasing order, the embedding dimension is  $M=70$ , which represents a time window of 70 years, b) First two empirical orthogonal functions (EOFs) of the Mediterranean SST time series c) time evolution of the mean annual SST of the Mediterranean Sea from 1854 to 2008 (black thin line) and the reconstructed time series (black thick line) are shown, the latter is based on SSA with a 70-year window, which retains the first two modes.

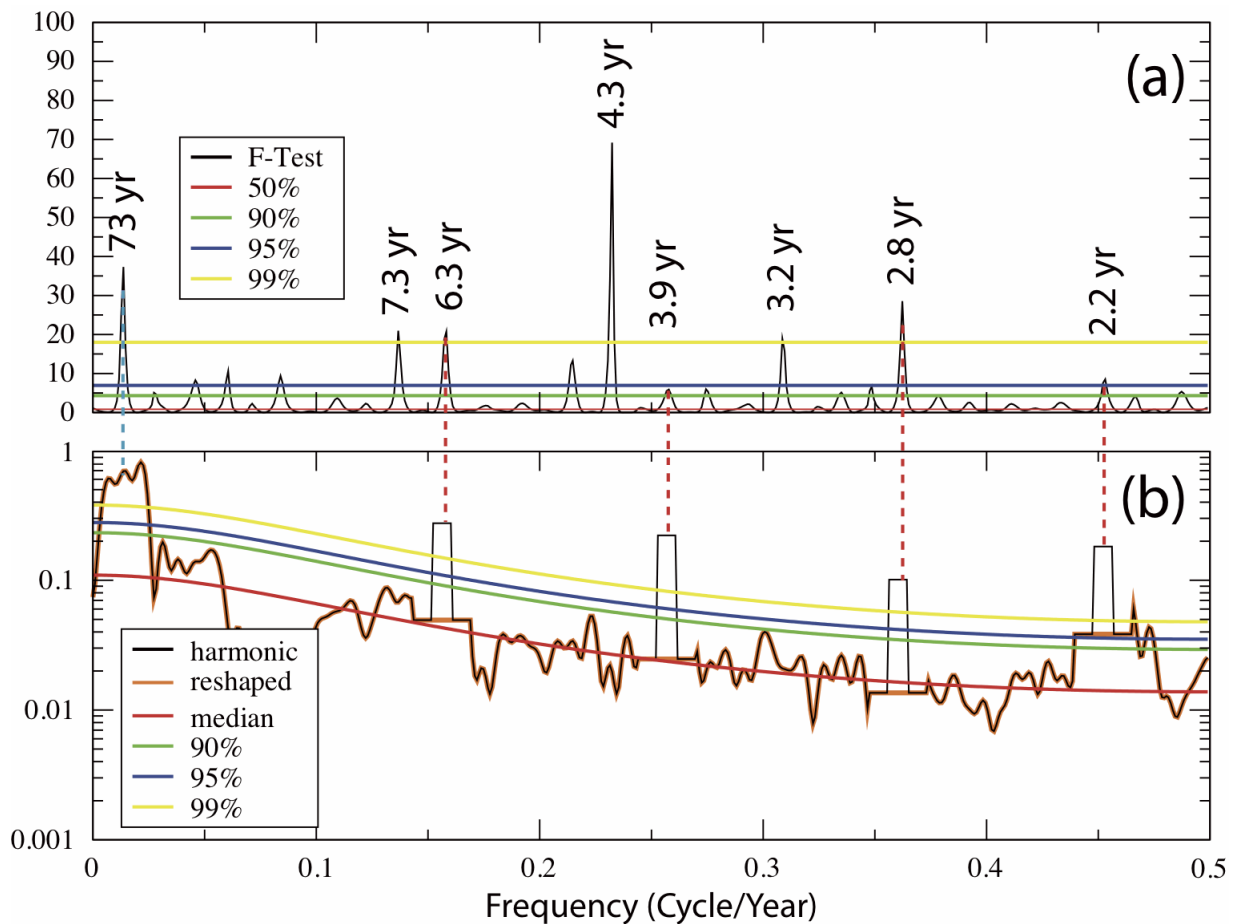


Fig. 9. Comparison between MTM spectra obtained by harmonic analysis test and adaptively weighted estimation against red noise background for the ERSST.v3 series of the Mediterranean Sea. Shown are (a) harmonic signal (variance ratio) F test with median, 90%, 95%, and 99% significance levels indicated and (b) reshaped (orange) versus unreshaped (black) adaptively weighted MTM spectrum based on  $p=2$  and  $K=3$ , and a 90% F test significance criterion for reshaping.

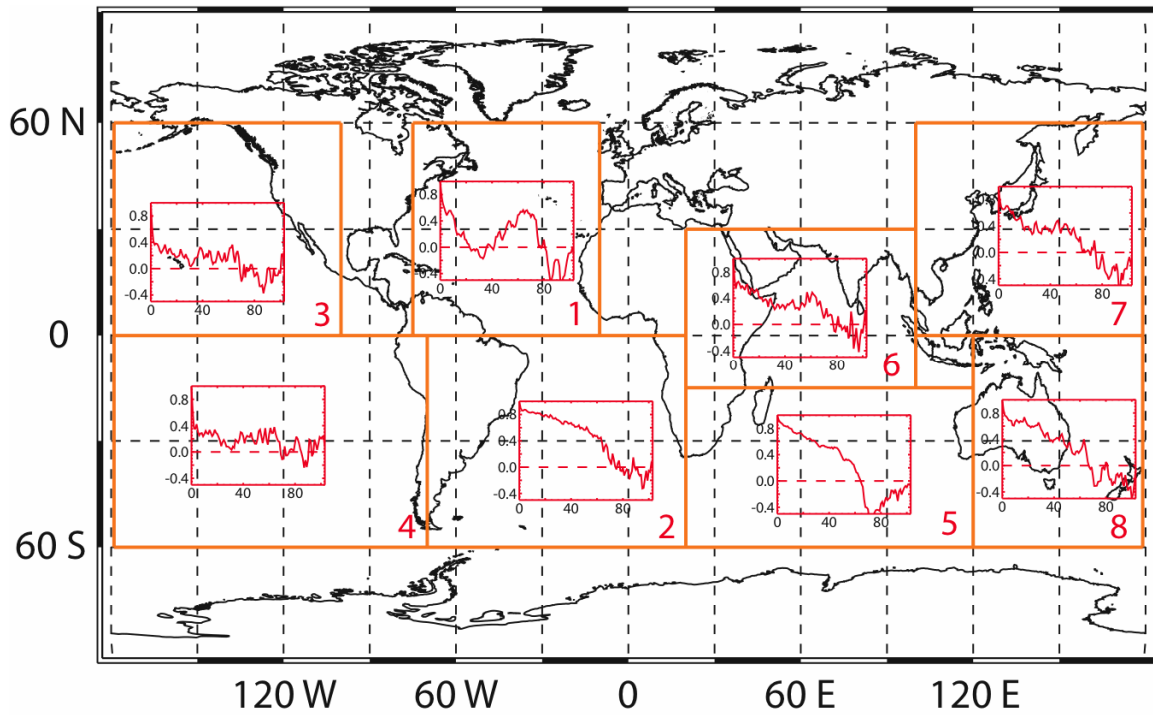


Fig. 10. Autocorrelation coefficients for different world ocean regions (based on HadISST data set). Units for abscissas are years.

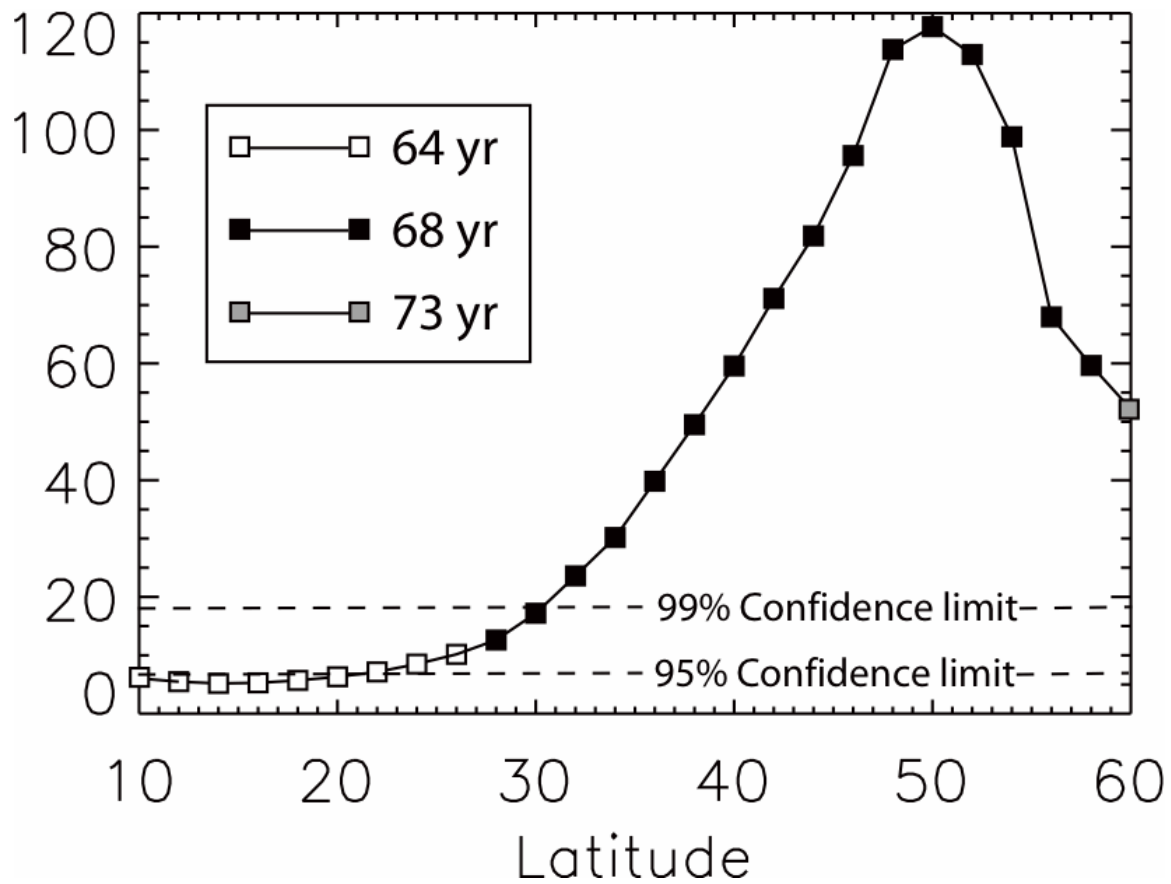


Fig. 11. Latitudinal variation of the amplitude of the harmonic signal in the North Atlantic (based on ERSSTV3 data). Symbols indicate the frequency where lines peak.

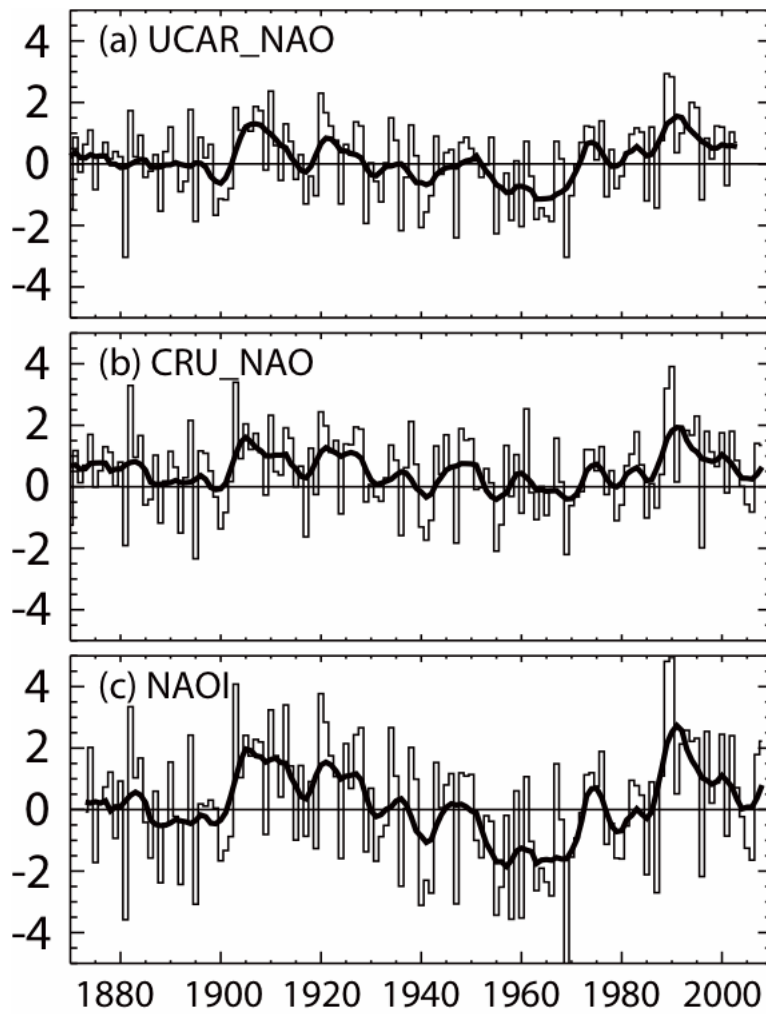


Fig. 12. Winter (JFM) NAO Index from different sources. (a) Climate Analysis Section of NCAR (Hurrell, 1995), (b) CRU-UEA, (c) Li and Wang (2003). The thin lines refer to yearly values while the thick lines refer to a 7 years Gaussian smoothing of the yearly values.

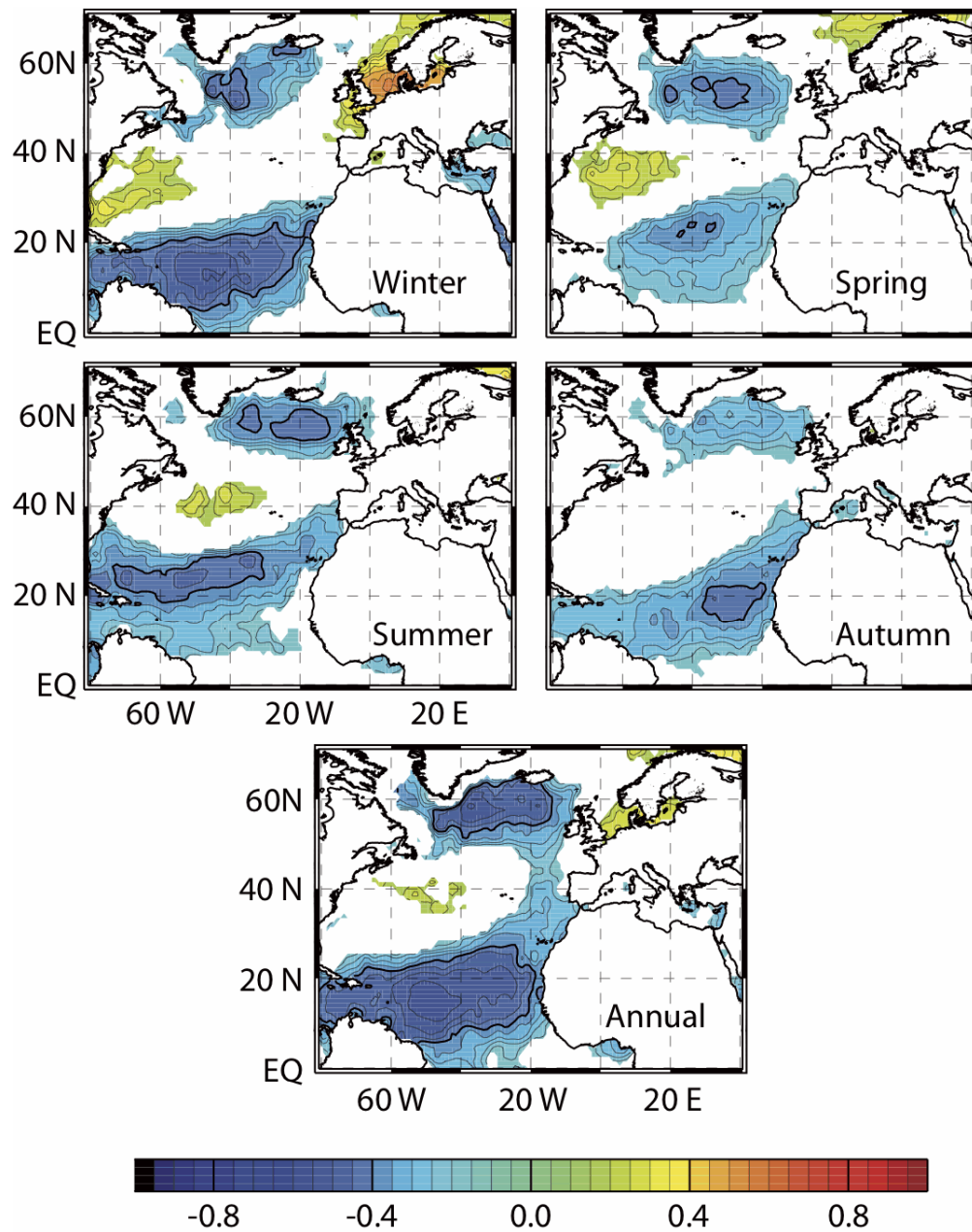


Fig. 13. Correlation maps between HadISST and NAOI. The thick contour line represents the -0.4 correlation level. Intervals between contour lines is 0.05. Colored regions represent areas where the 90% confidence level test has passed.

## Winter (Jan-Feb-Mar)

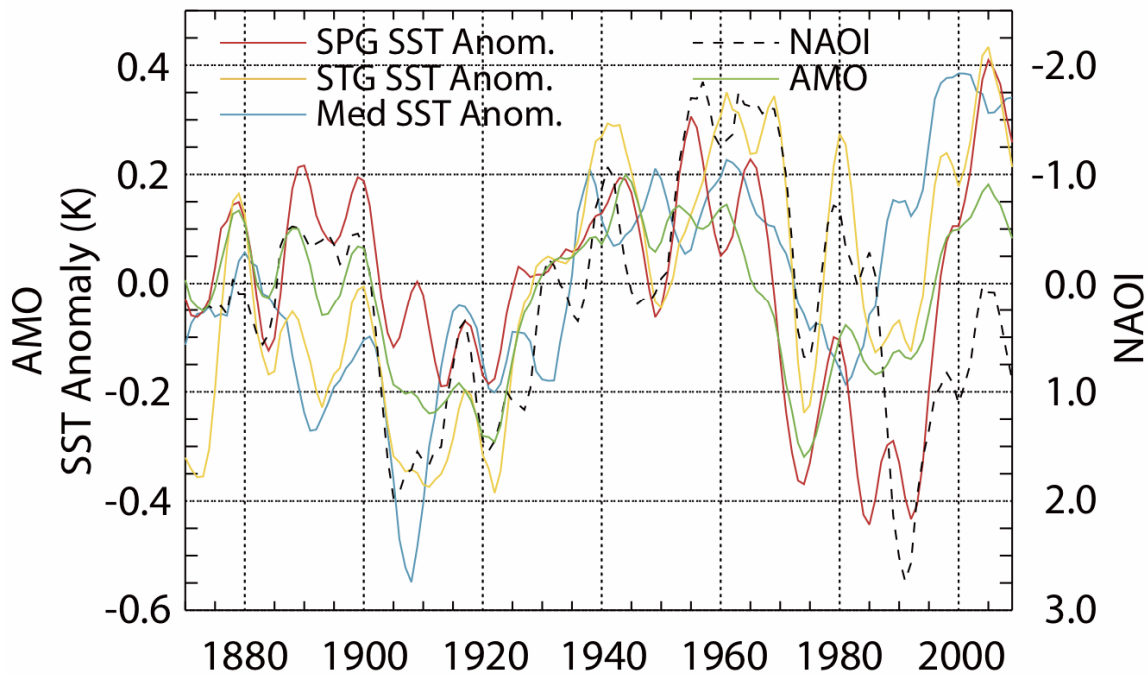


Fig. 14 Winter SST anomaly in the center of the Subpolar Gyre (SPG red solid line), in the subtropical gyre (STG yellow solid line) and in the Mediterranean Sea (Blue solid line) and AMO (green solid line). The dotted line represents the NAOI index (black). All the anomalies were calculated with respect to the mean of the entire period plotted in the figure using HadISST. NAOI has been plotted with the sign changed in order to better show the correlations with SSTs. All the time series have been filtered using a 7 year Gaussian filter. The center of the SPG and STG areas are defined as grid point where correlation is less or equal -0.4 (thick line in figure 13).



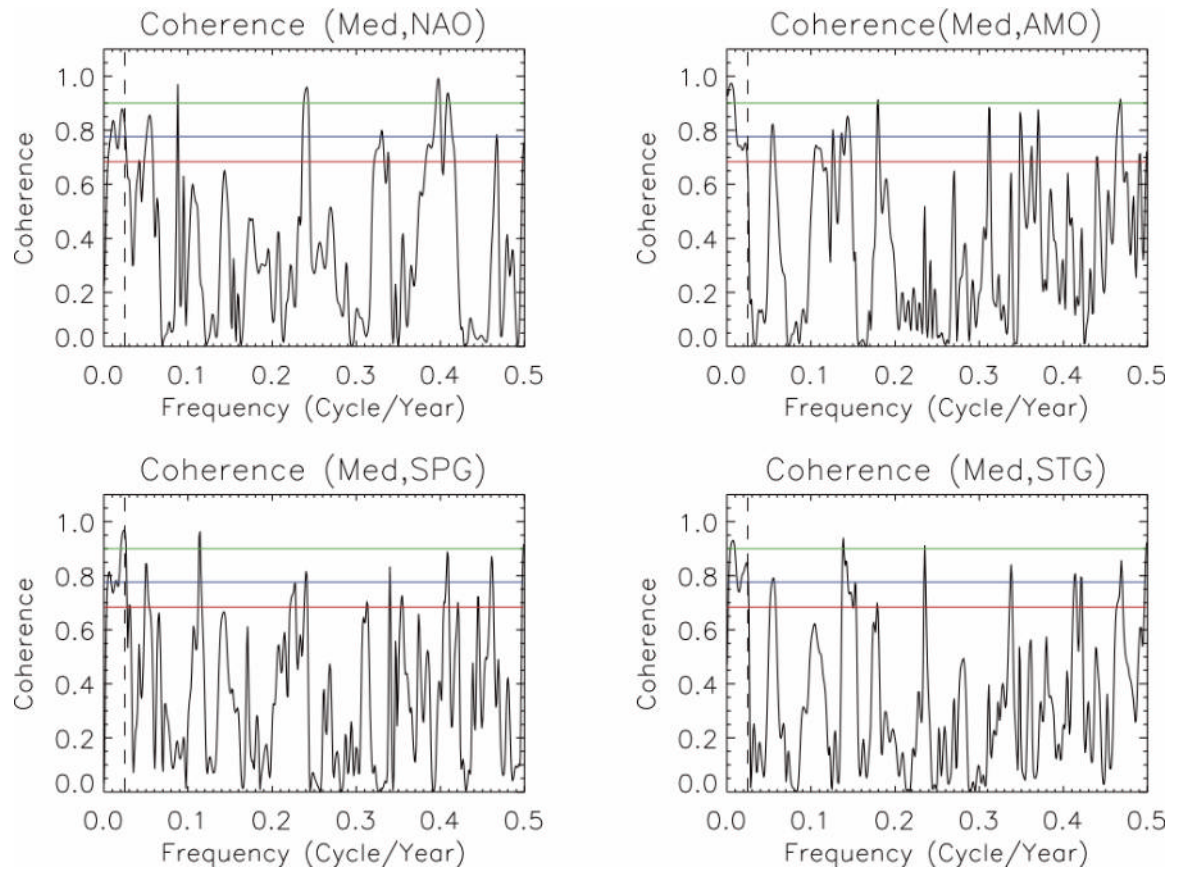


Fig. 15 Magnitude Squared Coherence estimation between Mediterranean SST and NAO (a), Mediterranean SST and AMO(b), Mediterranean SST and Sub Polar Gyre SST (c), Mediterranean SST and Sub Polar Gyre SST (d). Green , blue and red lines represent the 99%, 95% and 90% confidence limit respectively. The dotted vertical line represents the 40 years period.